

Search for B -Meson Decays to Two-body Final States with $a_0(980)$ Mesons

B. Aubert,¹ R. Barate,¹ D. Boutigny,¹ F. Couderc,¹ J.-M. Gaillard,¹ A. Hicheur,¹ Y. Karyotakis,¹ J. P. Lees,¹ V. Tisserand,¹ A. Zghiche,¹ A. Palano,² A. Pompili,² J. C. Chen,³ N. D. Qi,³ G. Rong,³ P. Wang,³ Y. S. Zhu,³ G. Eigen,⁴ I. Ofte,⁴ B. Stugu,⁴ G. S. Abrams,⁵ A. W. Borgland,⁵ A. B. Breon,⁵ D. N. Brown,⁵ J. Button-Shafer,⁵ R. N. Cahn,⁵ E. Charles,⁵ C. T. Day,⁵ M. S. Gill,⁵ A. V. Gritsan,⁵ Y. Groysman,⁵ R. G. Jacobsen,⁵ R. W. Kadel,⁵ J. Kadyk,⁵ L. T. Kerth,⁵ Yu. G. Kolomensky,⁵ G. Kukartsev,⁵ G. Lynch,⁵ L. M. Mir,⁵ P. J. Oddone,⁵ T. J. Orimoto,⁵ M. Pripstein,⁵ N. A. Roe,⁵ M. T. Ronan,⁵ V. G. Shelkov,⁵ W. A. Wenzel,⁵ M. Barrett,⁶ K. E. Ford,⁶ T. J. Harrison,⁶ A. J. Hart,⁶ C. M. Hawkes,⁶ S. E. Morgan,⁶ A. T. Watson,⁶ M. Fritsch,⁷ K. Goetzen,⁷ T. Held,⁷ H. Koch,⁷ B. Lewandowski,⁷ M. Pelizaeus,⁷ M. Steinke,⁷ J. T. Boyd,⁸ N. Chevalier,⁸ W. N. Cottingham,⁸ M. P. Kelly,⁸ T. E. Latham,⁸ F. F. Wilson,⁸ T. Cuhadar-Donszelmann,⁹ C. Hearty,⁹ N. S. Knecht,⁹ T. S. Mattison,⁹ J. A. McKenna,⁹ D. Thiessen,⁹ A. Khan,¹⁰ P. Kyberd,¹⁰ L. Teodorescu,¹⁰ A. E. Blinov,¹¹ V. E. Blinov,¹¹ V. P. Druzhinin,¹¹ V. B. Golubev,¹¹ V. N. Ivanchenko,¹¹ E. A. Kravchenko,¹¹ A. P. Onuchin,¹¹ S. I. Serednyakov,¹¹ Yu. I. Skovpen,¹¹ E. P. Solodov,¹¹ A. N. Yushkov,¹¹ D. Best,¹² M. Bruinsma,¹² M. Chao,¹² I. Eschrich,¹² D. Kirkby,¹² A. J. Lankford,¹² M. Mandelkern,¹² R. K. Mommsen,¹² W. Roethel,¹² D. P. Stoker,¹² C. Buchanan,¹³ B. L. Hartfiel,¹³ S. D. Foulkes,¹⁴ J. W. Gary,¹⁴ B. C. Shen,¹⁴ K. Wang,¹⁴ D. del Re,¹⁵ H. K. Hadavand,¹⁵ E. J. Hill,¹⁵ D. B. MacFarlane,¹⁵ H. P. Paar,¹⁵ Sh. Rahatlou,¹⁵ V. Sharma,¹⁵ J. W. Berryhill,¹⁶ C. Campagnari,¹⁶ B. Dahmes,¹⁶ S. L. Levy,¹⁶ O. Long,¹⁶ A. Lu,¹⁶ M. A. Mazur,¹⁶ J. D. Richman,¹⁶ W. Verkerke,¹⁶ T. W. Beck,¹⁷ A. M. Eisner,¹⁷ C. A. Heusch,¹⁷ W. S. Lockman,¹⁷ G. Nesom,¹⁷ T. Schalk,¹⁷ R. E. Schmitz,¹⁷ B. A. Schumm,¹⁷ A. Seiden,¹⁷ P. Spradlin,¹⁷ D. C. Williams,¹⁷ M. G. Wilson,¹⁷ J. Albert,¹⁸ E. Chen,¹⁸ G. P. Dubois-Felsmann,¹⁸ A. Dvoretzkii,¹⁸ D. G. Hitlin,¹⁸ I. Narsky,¹⁸ T. Piatenko,¹⁸ F. C. Porter,¹⁸ A. Ryd,¹⁸ A. Samuel,¹⁸ S. Yang,¹⁸ S. Jayatilake,¹⁹ G. Mancinelli,¹⁹ B. T. Meadows,¹⁹ M. D. Sokoloff,¹⁹ T. Abe,²⁰ F. Blanc,²⁰ P. Bloom,²⁰ S. Chen,²⁰ J. Destree,²⁰ W. T. Ford,²⁰ C. L. Lee,²⁰ U. Nauenberg,²⁰ A. Olivas,²⁰ P. Rankin,²⁰ J. G. Smith,²⁰ J. Zhang,²⁰ L. Zhang,²⁰ A. Chen,²¹ J. L. Harton,²¹ A. Soffer,²¹ W. H. Toki,²¹ R. J. Wilson,²¹ Q. L. Zeng,²¹ D. Altenburg,²² T. Brandt,²² J. Brose,²² M. Dickopp,²² E. Feltresi,²² A. Hauke,²² H. M. Lacker,²² R. Müller-Pfefferkorn,²² R. Nogowski,²² S. Otto,²² A. Petzold,²² J. Schubert,²² K. R. Schubert,²² R. Schwierz,²² B. Spaan,²² J. E. Sundermann,²² D. Bernard,²³ G. R. Bonneaud,²³ F. Brochard,²³ P. Grenier,²³ S. Schrenk,²³ Ch. Thiebaux,²³ G. Vasileiadis,²³ M. Verderi,²³ D. J. Bard,²⁴ P. J. Clark,²⁴ D. Lavin,²⁴ F. Muheim,²⁴ S. Playfer,²⁴ Y. Xie,²⁴ M. Andreotti,²⁵ V. Azzolini,²⁵ D. Bettoni,²⁵ C. Bozzi,²⁵ R. Calabrese,²⁵ G. Cibinetto,²⁵ E. Luppi,²⁵ M. Negrini,²⁵ L. Piemontese,²⁵ A. Sarti,²⁵ E. Treadwell,²⁶ R. Baldini-Ferrolli,²⁷ A. Calcaterra,²⁷ R. de Sangro,²⁷ G. Finocchiaro,²⁷ P. Patteri,²⁷ M. Piccolo,²⁷ A. Zallo,²⁷ A. Buzzo,²⁸ R. Capra,²⁸ R. Contri,²⁸ G. Crosetti,²⁸ M. Lo Vetere,²⁸ M. Macri,²⁸ M. R. Monge,²⁸ S. Passaggio,²⁸ C. Patrignani,²⁸ E. Robutti,²⁸ A. Santroni,²⁸ S. Tosi,²⁸ S. Bailey,²⁹ G. Brandenburg,²⁹ M. Morii,²⁹ E. Won,²⁹ R. S. Dubitzky,³⁰ U. Langenegger,³⁰ W. Bhimji,³¹ D. A. Bowerman,³¹ P. D. Dauncey,³¹ U. Egede,³¹ J. R. Gaillard,³¹ G. W. Morton,³¹ J. A. Nash,³¹ M. B. Nikolich,³¹ G. P. Taylor,³¹ M. J. Charles,³² G. J. Grenier,³² U. Mallik,³² J. Cochran,³³ H. B. Crawley,³³ J. Lamsa,³³ W. T. Meyer,³³ S. Prell,³³ E. I. Rosenberg,³³ J. Yi,³³ M. Davier,³⁴ G. Grosdidier,³⁴ A. Höcker,³⁴ S. Laplace,³⁴ F. Le Diberder,³⁴ V. Lepeltier,³⁴ A. M. Lutz,³⁴ T. C. Petersen,³⁴ S. Plaszczynski,³⁴ M. H. Schune,³⁴ L. Tantot,³⁴ G. Wormser,³⁴ C. H. Cheng,³⁵ D. J. Lange,³⁵ M. C. Simani,³⁵ D. M. Wright,³⁵ A. J. Bevan,³⁶ C. A. Chavez,³⁶ J. P. Coleman,³⁶ I. J. Forster,³⁶ J. R. Fry,³⁶ E. Gabathuler,³⁶ R. Gamet,³⁶ R. J. Parry,³⁶ D. J. Payne,³⁶ R. J. Sloane,³⁶ C. Touramanis,³⁶ J. J. Back,³⁷ * C. M. Cormack,³⁷ P. F. Harrison,³⁷ * F. Di Lodovico,³⁷ G. B. Mohanty,³⁷ * C. L. Brown,³⁸ G. Cowan,³⁸ R. L. Flack,³⁸ H. U. Flaecher,³⁸ M. G. Green,³⁸ P. S. Jackson,³⁸ T. R. McMahon,³⁸ S. Ricciardi,³⁸ F. Salvatore,³⁸ M. A. Winter,³⁸ D. Brown,³⁹ C. L. Davis,³⁹ J. Allison,⁴⁰ N. R. Barlow,⁴⁰ R. J. Barlow,⁴⁰ M. C. Hodgkinson,⁴⁰ G. D. Lafferty,⁴⁰ A. J. Lyon,⁴⁰ J. C. Williams,⁴⁰ A. Farbin,⁴¹ W. D. Hulsbergen,⁴¹ A. Jawahery,⁴¹ D. Kovalskyi,⁴¹ C. K. Lae,⁴¹ V. Lillard,⁴¹ D. A. Roberts,⁴¹ G. Blaylock,⁴² C. Dallapiccola,⁴² K. T. Flood,⁴² S. S. Hertzbach,⁴² R. Kofler,⁴² V. B. Koptchev,⁴² T. B. Moore,⁴² S. Saremi,⁴² H. Staengle,⁴² S. Willocq,⁴² R. Cowan,⁴³ G. Sciolla,⁴³ F. Taylor,⁴³ R. K. Yamamoto,⁴³ D. J. J. Mangeol,⁴⁴ P. M. Patel,⁴⁴ S. H. Robertson,⁴⁴ A. Lazzaro,⁴⁵ F. Palombo,⁴⁵ J. M. Bauer,⁴⁶ L. Cremaldi,⁴⁶ V. Eschenburg,⁴⁶ R. Godang,⁴⁶

R. Kroeger,⁴⁶ J. Reidy,⁴⁶ D. A. Sanders,⁴⁶ D. J. Summers,⁴⁶ H. W. Zhao,⁴⁶ S. Brunet,⁴⁷ D. Côté,⁴⁷ P. Taras,⁴⁷ H. Nicholson,⁴⁸ F. Fabozzi,⁴⁹,[†] C. Gatto,⁴⁹ L. Lista,⁴⁹ D. Monorchio,⁴⁹ P. Paolucci,⁴⁹ D. Piccolo,⁴⁹ C. Sciacca,⁴⁹ M. Baak,⁵⁰ H. Bulten,⁵⁰ G. Raven,⁵⁰ H. L. Snoek,⁵⁰ L. Wilden,⁵⁰ C. P. Jessop,⁵¹ J. M. LoSecco,⁵¹ T. A. Gabriel,⁵² T. Allmendinger,⁵³ B. Brau,⁵³ K. K. Gan,⁵³ K. Honscheid,⁵³ D. Hufnagel,⁵³ H. Kagan,⁵³ R. Kass,⁵³ T. Pulliam,⁵³ A. M. Rahimi,⁵³ R. Ter-Antonyan,⁵³ Q. K. Wong,⁵³ J. Brau,⁵⁴ R. Frey,⁵⁴ O. Igonkina,⁵⁴ C. T. Potter,⁵⁴ N. B. Sinev,⁵⁴ D. Strom,⁵⁴ E. Torrence,⁵⁴ F. Colecchia,⁵⁵ A. Dorigo,⁵⁵ F. Galeazzi,⁵⁵ M. Margoni,⁵⁵ M. Morandin,⁵⁵ M. Posocco,⁵⁵ M. Rotondo,⁵⁵ F. Simonetto,⁵⁵ R. Stroili,⁵⁵ G. Tiozzo,⁵⁵ C. Voci,⁵⁵ M. Benayoun,⁵⁶ H. Briand,⁵⁶ J. Chauveau,⁵⁶ P. David,⁵⁶ Ch. de la Vaissière,⁵⁶ L. Del Buono,⁵⁶ O. Hamon,⁵⁶ M. J. J. John,⁵⁶ Ph. Leruste,⁵⁶ J. Malcles,⁵⁶ J. Ocariz,⁵⁶ M. Pivk,⁵⁶ L. Roos,⁵⁶ S. T'Jampens,⁵⁶ G. Therin,⁵⁶ P. F. Manfredi,⁵⁷ V. Re,⁵⁷ P. K. Behera,⁵⁸ L. Gladney,⁵⁸ Q. H. Guo,⁵⁸ J. Panetta,⁵⁸ F. Anulli,^{27,59} M. Biasini,⁵⁹ I. M. Peruzzi,^{27,59} M. Pioppi,⁵⁹ C. Angelini,⁶⁰ G. Batignani,⁶⁰ S. Bettarini,⁶⁰ M. Bondioli,⁶⁰ F. Bucci,⁶⁰ G. Calderini,⁶⁰ M. Carpinelli,⁶⁰ F. Forti,⁶⁰ M. A. Giorgi,⁶⁰ A. Lusiani,⁶⁰ G. Marchiori,⁶⁰ F. Martinez-Vidal,⁶⁰,[‡] M. Morganti,⁶⁰ N. Neri,⁶⁰ E. Paoloni,⁶⁰ M. Rama,⁶⁰ G. Rizzo,⁶⁰ F. Sandrelli,⁶⁰ J. Walsh,⁶⁰ M. Haire,⁶¹ D. Judd,⁶¹ K. Paick,⁶¹ D. E. Wagoner,⁶¹ N. Danielson,⁶² P. Elmer,⁶² Y. P. Lau,⁶² C. Lu,⁶² V. Miftakov,⁶² J. Olsen,⁶² A. J. S. Smith,⁶² A. V. Telnov,⁶² F. Bellini,⁶³ G. Cavoto,^{62,63} R. Faccini,⁶³ F. Ferrarotto,⁶³ F. Ferroni,⁶³ M. Gaspero,⁶³ L. Li Gioi,⁶³ M. A. Mazzoni,⁶³ S. Morganti,⁶³ M. Pierini,⁶³ G. Piredda,⁶³ F. Safai Tehrani,⁶³ C. Voena,⁶³ S. Christ,⁶⁴ G. Wagner,⁶⁴ R. Waldi,⁶⁴ T. Adye,⁶⁵ N. De Groot,⁶⁵ B. Franek,⁶⁵ N. I. Geddes,⁶⁵ G. P. Gopal,⁶⁵ E. O. Olaiya,⁶⁵ R. Aleksan,⁶⁶ S. Emery,⁶⁶ A. Gaidot,⁶⁶ S. F. Ganzhur,⁶⁶ P.-F. Giraud,⁶⁶ G. Hamel de Monchenault,⁶⁶ W. Kozanecki,⁶⁶ M. Langer,⁶⁶ M. Legendre,⁶⁶ G. W. London,⁶⁶ B. Mayer,⁶⁶ G. Schott,⁶⁶ G. Vasseur,⁶⁶ Ch. Yèche,⁶⁶ M. Zito,⁶⁶ M. V. Purohit,⁶⁷ A. W. Weidemann,⁶⁷ J. R. Wilson,⁶⁷ F. X. Yumiceva,⁶⁷ D. Aston,⁶⁸ R. Bartoldus,⁶⁸ N. Berger,⁶⁸ A. M. Boyarski,⁶⁸ O. L. Buchmueller,⁶⁸ R. Claus,⁶⁸ M. R. Convery,⁶⁸ M. Cristinziani,⁶⁸ G. De Nardo,⁶⁸ D. Dong,⁶⁸ J. Dorfan,⁶⁸ D. Dujmic,⁶⁸ W. Dunwoodie,⁶⁸ E. E. Elsen,⁶⁸ S. Fan,⁶⁸ R. C. Field,⁶⁸ T. Glanzman,⁶⁸ S. J. Gowdy,⁶⁸ T. Hadig,⁶⁸ V. Halyo,⁶⁸ C. Hast,⁶⁸ T. Hryn'ova,⁶⁸ W. R. Innes,⁶⁸ M. H. Kelsey,⁶⁸ P. Kim,⁶⁸ M. L. Kocian,⁶⁸ D. W. G. S. Leith,⁶⁸ J. Libby,⁶⁸ S. Luitz,⁶⁸ V. Luth,⁶⁸ H. L. Lynch,⁶⁸ H. Marsiske,⁶⁸ R. Messner,⁶⁸ D. R. Muller,⁶⁸ C. P. O'Grady,⁶⁸ V. E. Ozcan,⁶⁸ A. Perazzo,⁶⁸ M. Perl,⁶⁸ S. Petrak,⁶⁸ B. N. Ratcliff,⁶⁸ A. Roodman,⁶⁸ A. A. Salnikov,⁶⁸ R. H. Schindler,⁶⁸ J. Schwiening,⁶⁸ G. Simi,⁶⁸ A. Snyder,⁶⁸ A. Soha,⁶⁸ J. Stelzer,⁶⁸ D. Su,⁶⁸ M. K. Sullivan,⁶⁸ J. Va'vra,⁶⁸ S. R. Wagner,⁶⁸ M. Weaver,⁶⁸ A. J. R. Weinstein,⁶⁸ W. J. Wisniewski,⁶⁸ M. Wittgen,⁶⁸ D. H. Wright,⁶⁸ A. K. Yarritu,⁶⁸ C. C. Young,⁶⁸ P. R. Burchat,⁶⁹ A. J. Edwards,⁶⁹ T. I. Meyer,⁶⁹ B. A. Petersen,⁶⁹ C. Roat,⁶⁹ S. Ahmed,⁷⁰ M. S. Alam,⁷⁰ J. A. Ernst,⁷⁰ M. A. Saeed,⁷⁰ M. Saleem,⁷⁰ F. R. Wappler,⁷⁰ W. Bugg,⁷¹ M. Krishnamurthy,⁷¹ S. M. Spanier,⁷¹ R. Eckmann,⁷² H. Kim,⁷² J. L. Ritchie,⁷² A. Satpathy,⁷² R. F. Schwitters,⁷² J. M. Izen,⁷³ I. Kitayama,⁷³ X. C. Lou,⁷³ S. Ye,⁷³ F. Bianchi,⁷⁴ M. Bona,⁷⁴ F. Gallo,⁷⁴ D. Gamba,⁷⁴ C. Borean,⁷⁵ L. Bosisio,⁷⁵ C. Cartaro,⁷⁵ F. Cossutti,⁷⁵ G. Della Ricca,⁷⁵ S. Dittongo,⁷⁵ S. Grancagnolo,⁷⁵ L. Lanceri,⁷⁵ P. Poropat,⁷⁵,[§] L. Vitale,⁷⁵ G. Vuagnin,⁷⁵ R. S. Panvini,⁷⁶ Sw. Banerjee,⁷⁷ C. M. Brown,⁷⁷ D. Fortin,⁷⁷ P. D. Jackson,⁷⁷ R. Kowalewski,⁷⁷ J. M. Roney,⁷⁷ R. J. Sobie,⁷⁷ H. R. Band,⁷⁸ S. Dasu,⁷⁸ M. Datta,⁷⁸ A. M. Eichenbaum,⁷⁸ M. Graham,⁷⁸ J. J. Hollar,⁷⁸ J. R. Johnson,⁷⁸ P. E. Kutter,⁷⁸ H. Li,⁷⁸ R. Liu,⁷⁸ A. Mihalyi,⁷⁸ A. K. Mohapatra,⁷⁸ Y. Pan,⁷⁸ R. Prepost,⁷⁸ A. E. Rubin,⁷⁸ S. J. Sekula,⁷⁸ P. Tan,⁷⁸ J. H. von Wimmersperg-Toeller,⁷⁸ J. Wu,⁷⁸ S. L. Wu,⁷⁸ Z. Yu,⁷⁸ M. G. Greene,⁷⁹ and H. Neal⁷⁹

(The BABAR Collaboration)

¹Laboratoire de Physique des Particules, F-74941 Annecy-le-Vieux, France

²Università di Bari, Dipartimento di Fisica and INFN, I-70126 Bari, Italy

³Institute of High Energy Physics, Beijing 100039, China

⁴University of Bergen, Inst. of Physics, N-5007 Bergen, Norway

⁵Lawrence Berkeley National Laboratory and University of California, Berkeley, CA 94720, USA

⁶University of Birmingham, Birmingham, B15 2TT, United Kingdom

⁷Ruhr Universität Bochum, Institut für Experimentalphysik 1, D-44780 Bochum, Germany

⁸University of Bristol, Bristol BS8 1TL, United Kingdom

⁹University of British Columbia, Vancouver, BC, Canada V6T 1Z1

¹⁰Brunel University, Uxbridge, Middlesex UB8 3PH, United Kingdom

¹¹Budker Institute of Nuclear Physics, Novosibirsk 630090, Russia

¹²University of California at Irvine, Irvine, CA 92697, USA

¹³University of California at Los Angeles, Los Angeles, CA 90024, USA

¹⁴University of California at Riverside, Riverside, CA 92521, USA

¹⁵University of California at San Diego, La Jolla, CA 92093, USA

¹⁶University of California at Santa Barbara, Santa Barbara, CA 93106, USA

- ¹⁷University of California at Santa Cruz, Institute for Particle Physics, Santa Cruz, CA 95064, USA
- ¹⁸California Institute of Technology, Pasadena, CA 91125, USA
- ¹⁹University of Cincinnati, Cincinnati, OH 45221, USA
- ²⁰University of Colorado, Boulder, CO 80309, USA
- ²¹Colorado State University, Fort Collins, CO 80523, USA
- ²²Technische Universität Dresden, Institut für Kern- und Teilchenphysik, D-01062 Dresden, Germany
- ²³Ecole Polytechnique, LLR, F-91128 Palaiseau, France
- ²⁴University of Edinburgh, Edinburgh EH9 3JZ, United Kingdom
- ²⁵Università di Ferrara, Dipartimento di Fisica and INFN, I-44100 Ferrara, Italy
- ²⁶Florida A&M University, Tallahassee, FL 32307, USA
- ²⁷Laboratori Nazionali di Frascati dell'INFN, I-00044 Frascati, Italy
- ²⁸Università di Genova, Dipartimento di Fisica and INFN, I-16146 Genova, Italy
- ²⁹Harvard University, Cambridge, MA 02138, USA
- ³⁰Universität Heidelberg, Physikalisches Institut, Philosophenweg 12, D-69120 Heidelberg, Germany
- ³¹Imperial College London, London, SW7 2AZ, United Kingdom
- ³²University of Iowa, Iowa City, IA 52242, USA
- ³³Iowa State University, Ames, IA 50011-3160, USA
- ³⁴Laboratoire de l'Accélérateur Linéaire, F-91898 Orsay, France
- ³⁵Lawrence Livermore National Laboratory, Livermore, CA 94550, USA
- ³⁶University of Liverpool, Liverpool L69 7ZE, United Kingdom
- ³⁷Queen Mary, University of London, E1 4NS, United Kingdom
- ³⁸University of London, Royal Holloway and Bedford New College, Egham, Surrey TW20 0EX, United Kingdom
- ³⁹University of Louisville, Louisville, KY 40292, USA
- ⁴⁰University of Manchester, Manchester M13 9PL, United Kingdom
- ⁴¹University of Maryland, College Park, MD 20742, USA
- ⁴²University of Massachusetts, Amherst, MA 01003, USA
- ⁴³Massachusetts Institute of Technology, Laboratory for Nuclear Science, Cambridge, MA 02139, USA
- ⁴⁴McGill University, Montréal, QC, Canada H3A 2T8
- ⁴⁵Università di Milano, Dipartimento di Fisica and INFN, I-20133 Milano, Italy
- ⁴⁶University of Mississippi, University, MS 38677, USA
- ⁴⁷Université de Montréal, Laboratoire René J. A. Lévesque, Montréal, QC, Canada H3C 3J7
- ⁴⁸Mount Holyoke College, South Hadley, MA 01075, USA
- ⁴⁹Università di Napoli Federico II, Dipartimento di Scienze Fisiche and INFN, I-80126, Napoli, Italy
- ⁵⁰NIKHEF, National Institute for Nuclear Physics and High Energy Physics, NL-1009 DB Amsterdam, The Netherlands
- ⁵¹University of Notre Dame, Notre Dame, IN 46556, USA
- ⁵²Oak Ridge National Laboratory, Oak Ridge, TN 37831, USA
- ⁵³Ohio State University, Columbus, OH 43210, USA
- ⁵⁴University of Oregon, Eugene, OR 97403, USA
- ⁵⁵Università di Padova, Dipartimento di Fisica and INFN, I-35131 Padova, Italy
- ⁵⁶Universités Paris VI et VII, Laboratoire de Physique Nucléaire et de Hautes Energies, F-75252 Paris, France
- ⁵⁷Università di Pavia, Dipartimento di Eletttronica and INFN, I-27100 Pavia, Italy
- ⁵⁸University of Pennsylvania, Philadelphia, PA 19104, USA
- ⁵⁹Università di Perugia, Dipartimento di Fisica and INFN, I-06100 Perugia, Italy
- ⁶⁰Università di Pisa, Dipartimento di Fisica, Scuola Normale Superiore and INFN, I-56127 Pisa, Italy
- ⁶¹Prairie View A&M University, Prairie View, TX 77446, USA
- ⁶²Princeton University, Princeton, NJ 08544, USA
- ⁶³Università di Roma La Sapienza, Dipartimento di Fisica and INFN, I-00185 Roma, Italy
- ⁶⁴Universität Rostock, D-18051 Rostock, Germany
- ⁶⁵Rutherford Appleton Laboratory, Chilton, Didcot, Oxon, OX11 0QX, United Kingdom
- ⁶⁶DSM/Dapnia, CEA/Saclay, F-91191 Gif-sur-Yvette, France
- ⁶⁷University of South Carolina, Columbia, SC 29208, USA
- ⁶⁸Stanford Linear Accelerator Center, Stanford, CA 94309, USA
- ⁶⁹Stanford University, Stanford, CA 94305-4060, USA
- ⁷⁰State Univ. of New York, Albany, NY 12222, USA
- ⁷¹University of Tennessee, Knoxville, TN 37996, USA
- ⁷²University of Texas at Austin, Austin, TX 78712, USA
- ⁷³University of Texas at Dallas, Richardson, TX 75083, USA
- ⁷⁴Università di Torino, Dipartimento di Fisica Sperimentale and INFN, I-10125 Torino, Italy
- ⁷⁵Università di Trieste, Dipartimento di Fisica and INFN, I-34127 Trieste, Italy
- ⁷⁶Vanderbilt University, Nashville, TN 37235, USA
- ⁷⁷University of Victoria, Victoria, BC, Canada V8W 3P6
- ⁷⁸University of Wisconsin, Madison, WI 53706, USA
- ⁷⁹Yale University, New Haven, CT 06511, USA
- (Dated: July 27, 2021)

We present a search for B decays to charmless final states involving charged or neutral a_0 mesons. The data sample corresponds to 89 million $B\bar{B}$ pairs collected with the *BABAR* detector operating at the PEP-II asymmetric-energy B Factory at SLAC. We find no significant signals and determine the following 90% C.L. upper limits: $\mathcal{B}(B^0 \rightarrow a_0^- \pi^+) < 5.1 \times 10^{-6}$, $\mathcal{B}(B^0 \rightarrow a_0^- K^+) < 2.1 \times 10^{-6}$, $\mathcal{B}(B^- \rightarrow a_0^- \bar{K}^0) < 3.9 \times 10^{-6}$, $\mathcal{B}(B^+ \rightarrow a_0^0 \pi^+) < 5.8 \times 10^{-6}$, $\mathcal{B}(B^+ \rightarrow a_0^0 K^+) < 2.5 \times 10^{-6}$, and $\mathcal{B}(B^0 \rightarrow a_0^0 K^0) < 7.8 \times 10^{-6}$, where in all cases \mathcal{B} indicates the product of branching fractions for $B \rightarrow a_0 X$ and $a_0 \rightarrow \eta\pi$, where X indicates K or π .

PACS numbers: 13.25.Hw, 12.15.Hh, 11.30.Er

We report results on measurements of B -meson decays to charmless final states with $a_0(980)$ mesons [1]. Both experimentally and theoretically, most work in charmless two-body B decays has involved states with only pseudoscalar and vector mesons. The only charmless B decay involving scalar mesons that has been observed is $B \rightarrow f_0(980)K$ [2]. There have been no previously published searches for B decays to final states with a_0 mesons. In this paper we search for the decays $B \rightarrow a_0\pi$, $B \rightarrow a_0K$, and $B \rightarrow a_0K^0$ for both charged and neutral a_0 mesons. These measurements should provide information both for B decays to scalar mesons and the nature of those mesons.

Some specific predictions can be made for the decays $B \rightarrow a_0\pi^\pm$ if factorization is assumed and if the decay is a tree or penguin (loop) process. The dominant such process is shown in Fig. 1(a). The companion tree process, shown in Fig. 1(b), is expected to be greatly suppressed, since the virtual W cannot produce an a_0 meson [4]. This is a firm prediction of the Standard Model because the weak current has a G -parity even vector part and a G -parity odd axial-vector part. The latter can produce an axial-vector or pseudoscalar particle while the former produces a vector particle, but neither can produce a G -parity odd scalar meson. Penguin processes such as shown in Fig. 1(c) are allowed, but are suppressed relative to the tree processes. Thus the decay $B \rightarrow a_0\pi^\pm$ is expected to be “self-tagging” (the charge of the pion identifies the B flavor). The decays with a kaon in the final state should be dominated by penguin processes (Fig. 1d); however, there is a cancellation between two terms in the penguin amplitudes for these decays [5], which leads to a prediction that the branching fraction should be rather small. The diagrams for neutral B decays involving a_0^0 mesons are similar to those shown in Fig. 1.

The nature of the a_0 is still not well understood. It is thought to be a $q\bar{q}$ state with a possible admixture of a $K\bar{K}$ bound-state component due to the proximity to the $K\bar{K}$ threshold [6, 7]. The a_0 mass is known to be about 985 MeV and the dominant decay mode is $a_0 \rightarrow \eta\pi$ [6], which is the mode used in the present analysis. A recent analysis [8] that uses this $\eta\pi$ decay channel finds a Breit-Wigner width of (71 ± 7) MeV, with no better fit obtained when the more correct Flatté shape [9] is used. Also since the branching fraction for $a_0 \rightarrow \eta\pi$ is

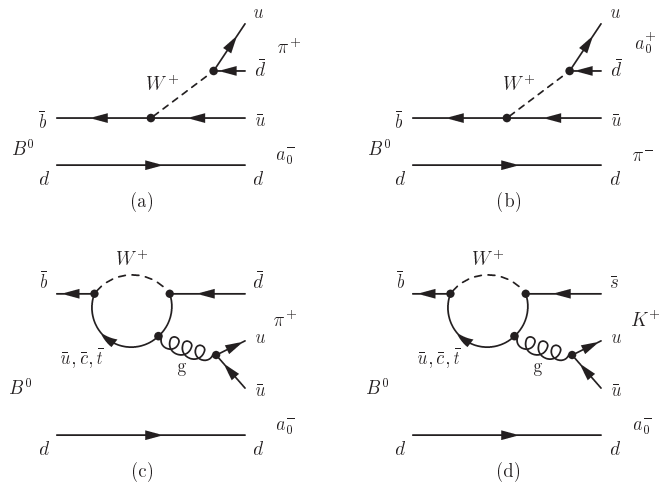


FIG. 1: Feynman diagrams for decays involving charged a_0 mesons: (a) dominant and (b) G -parity-suppressed tree diagrams for $B^0 \rightarrow a_0^\mp \pi^\pm$, (c) penguin diagram for the same decay mode, and (d) penguin diagram for the decay $B^0 \rightarrow a_0^- K^+$.

not well known, we report the product branching fraction $\mathcal{B}(B \rightarrow a_0 X) \times \mathcal{B}(a_0 \rightarrow \eta\pi)$, where X indicates K or π .

The results presented here are based on data collected with the *BABAR* detector [10] at the PEP-II asymmetric e^+e^- collider located at the Stanford Linear Accelerator Center. An integrated luminosity of 81.9 fb^{-1} , corresponding to 88.9 ± 1.0 million $B\bar{B}$ pairs, was recorded at the $\Upsilon(4S)$ resonance (center-of-mass energy $\sqrt{s} = 10.58$ GeV).

The track parameters of charged particles are measured by a combination of a silicon vertex tracker, with five layers of double-sided silicon sensors, and a 40-layer central drift chamber, both operating in the 1.5-T magnetic field of a superconducting solenoid. We identify photons and electrons using a CsI(Tl) electromagnetic calorimeter (EMC). Further charged particle identification (PID) is provided by the average energy loss (dE/dx) in the tracking devices and by an internally-reflecting, ring-imaging Cherenkov detector (DIRC) covering the central region.

We select a_0 candidates from the decay channel $a_0 \rightarrow \eta\pi$ with the decays $\eta \rightarrow \gamma\gamma$ ($\eta_{\gamma\gamma}$) and $\eta \rightarrow \pi^+\pi^-\pi^0$ ($\eta_{3\pi}$). We apply the following requirements on the in-

variant masses (in MeV) relevant here: $500 < m_{\gamma\gamma} < 585$ for $\eta_{\gamma\gamma}$, $535 < m_{\pi\pi\pi} < 560$ for $\eta_{3\pi}$, $120 < m_{\gamma\gamma} < 150$ for π^0 , and $775 < m_{\eta\pi} < 1175$ for $a_0 \rightarrow \eta\pi$. These requirements are typically quite loose compared with typical resolutions in order to achieve high efficiency and retain sufficient sidebands to characterize the background for subsequent fitting. We reconstruct K_s^0 candidates through the $K_s^0 \rightarrow \pi^+\pi^-$ decay; to obtain a low-background, well-understood K_s^0 sample, we require $488 < m_{\pi\pi} < 508$ MeV, the three-dimensional flight distance from the event primary vertex to be greater than 2 mm, and the angle between flight and momentum vectors, in the plane perpendicular to the beam direction, to be less than 40 mrad.

We make several PID requirements to ensure the identity of the pions and kaons. Secondary tracks in $\eta_{3\pi}$ candidates must have measured DIRC, dE/dx , and EMC outputs consistent with pions. For the decays $B \rightarrow a_0 h^+$ [3], where h^+ indicates a charged pion or kaon, the particle h^+ must have an associated DIRC signal with a Cherenkov angle within 3.5 standard deviations of the expected value for either a π^\pm or K^\pm hypothesis (we describe below the separation between the two hypotheses).

A B -meson candidate is characterized kinematically by the energy-substituted mass $m_{\text{ES}} = [(\frac{1}{2}s + \mathbf{p}_0 \cdot \mathbf{p}_B)^2 / E_0^2 - \mathbf{p}_B^2]^{\frac{1}{2}}$ and energy difference $\Delta E = E_B^* - \frac{1}{2}\sqrt{s}$, where (E_B, \mathbf{p}_B) and (E_0, \mathbf{p}_0) are the four vectors of the B -candidate and the initial electron-positron system, respectively. The asterisk denotes the $\Upsilon(4S)$ frame, and s is the square of the invariant mass of the electron-positron system. The ΔE (m_{ES}) resolution is about 40 MeV (3.0 MeV). We require $|\Delta E| \leq 0.2$ GeV and $5.2 \leq m_{\text{ES}} \leq 5.29$ GeV.

Backgrounds arise primarily from random combinations in continuum $e^+e^- \rightarrow q\bar{q}$ ($q = u, d, s, c$) events. We reduce these by using the angle θ_T between the thrust axis of the B candidate in the $\Upsilon(4S)$ frame and that of the rest of the charged tracks and neutral clusters in the event. The distribution of $|\cos \theta_T|$ is sharply peaked near 1.0 for combinations drawn from jet-like $q\bar{q}$ pairs, and nearly uniform for B -meson decays. We require $|\cos \theta_T| < 0.9$ for the $a_0 K_s^0$ decay modes. Based on a Monte Carlo study in which the relative branching fraction uncertainty is minimized, we tighten this requirement for the higher-background $a_0 h$ channels: 0.8 for $a_0^-(\eta_{3\pi})h^+$, 0.7 for $a_0^-(\eta_{\gamma\gamma})h^+$ and $a_0^0(\eta_{3\pi})h^+$, and 0.6 for $a_0^0(\eta_{\gamma\gamma})h^+$. We also use, in the fit described below, a Fisher discriminant \mathcal{F} that combines the angles with respect to the beam axis of the B momentum and B thrust axis (in the $\Upsilon(4S)$ frame), and moments describing the energy flow about the B thrust axis [11].

For the $\eta \rightarrow \gamma\gamma$ modes we use additional event-selection criteria to further reduce backgrounds from charmless B decay modes such as $B \rightarrow K^*\gamma$ and $B \rightarrow \eta K^*$. We require $|\cos \theta_{\text{dec}}^\eta| \leq 0.86$, where θ_{dec}^η is the η decay angle, the angle of the photons in the η rest frame

with respect to the boost direction from the B to that frame. We also require $\cos \theta_{\text{dec}}^{a_0} \leq 0.8$, where $\theta_{\text{dec}}^{a_0}$ is the a_0 decay angle, defined similarly to θ_{dec}^η , with sign such that high-momentum η mesons populate the region near +1. These additional requirements reduce the $B\bar{B}$ background by a factor of 2–4, depending on the decay mode. From Monte Carlo (MC) simulation [12] we estimate that the residual charmless $B\bar{B}$ background is less than one event for all decays except $a_0^-(\eta_{\gamma\gamma})\bar{K}^0$ (the notation indicates the decay mode of the η used in reconstructing the a_0) and $a_0^0(\eta_{\gamma\gamma})h^+$, where we include in the fit a $B\bar{B}$ component, that we find to be less than 0.5% of the total sample in both cases.

We obtain yields and branching fractions from extended unbinned maximum-likelihood fits, with input observables ΔE , m_{ES} , \mathcal{F} , $m_{\eta\pi}$, and for charged modes the PID variables S_π and S_K ; the last quantities are the number of standard deviations between the measured Cherenkov angle and the expectation for pions and kaons.

For each event i , hypothesis j (signal, continuum background, $B\bar{B}$ background), and, for the $a_0 h^+$ decays, flavor k , we define the probability density function (PDF)

$$\mathcal{P}_{jk}^i = \mathcal{P}_j(m_{\text{ES}}^i) \mathcal{P}_j(\Delta E_k^i, S_k^i) \mathcal{P}_j(\mathcal{F}^i) \mathcal{P}_j(m_{\eta\pi}^i). \quad (1)$$

The term in brackets for S pertains to the $a_0 h^+$ modes. The absence of correlations among observables (except between ΔE and S , which both depend on the momentum of the particle h^+) in the background \mathcal{P}_{jk}^i , is confirmed in the (background-dominated) data samples entering the fit. For the signal component, we correct for effects due to the neglect of small correlations (more details are provided in the systematics discussion below). The likelihood function is

$$\mathcal{L} = \exp\left(-\sum_{j,k} Y_{jk}\right) \prod_i^N \left[\sum_{j,k} Y_{jk} \mathcal{P}_{jk}^i \right], \quad (2)$$

where Y_{jk} is the yield of events of hypothesis j and flavor k that we find by maximizing \mathcal{L} , and N is the number of events in the sample.

We determine the PDF parameters from simulation for the signal and $B\bar{B}$ background components, and initial values of the continuum background parameters from $(m_{\text{ES}}, \Delta E)$ sideband data. We parameterize each of the functions $\mathcal{P}_{\text{sig}}(m_{\text{ES}})$, $\mathcal{P}_{\text{sig}}(\Delta E_k)$, $\mathcal{P}_j(\mathcal{F})$, and $\mathcal{P}_j(S_k)$ with either a Gaussian function, the sum of two Gaussian functions or an asymmetric Gaussian function, as required to describe the distribution. The component of $\mathcal{P}_j(m_{\eta\pi})$ which represents real a_0 mesons in the combinatorial background is described with the same Breit-Wigner parameters as are used for signal. Slowly varying distributions (a_0 candidate mass and ΔE for combinatoric background) are represented by second order Chebyshev polynomials. The $q\bar{q}$ combinatoric background in m_{ES} is described by the function $f(x) =$

$x\sqrt{1-x^2}\exp[-\xi(1-x^2)]$, with $x \equiv 2m_{\text{ES}}/\sqrt{s}$ and free parameter ξ ; for $B\bar{B}$ background, we add a Gaussian function to the quantity $f(x)$. Large control samples of $B \rightarrow D\pi$ decays of topology similar to the signal are used to verify the simulated resolutions in ΔE and m_{ES} . Where the control data samples reveal differences from MC, we shift or scale the resolution used in the likelihood fits. Examples of many of these PDF shapes from a very similar analysis are shown in Ref. [11]. Additionally, the Breit-Wigner signal parameters for the a_0 mass and width are determined from an inclusive dataset that is much larger than the sample used for this analysis. The widths are consistent with expectations from the natural-width values of Ref. [8].

In Table I we show for each decay mode the measured product branching fraction, together with the quantities entering into its determination. In order to account for the uncertainties in the background PDF descriptions, we include as free parameters in the fit, in addition to the signal and background yields, the principle parameters describing the background PDFs: slopes for the polynomial shape for the ΔE and a_0 mass distributions, the parameter ξ used in the m_{ES} description, and three parameters describing the asymmetric Gaussian function for \mathcal{F} . For calculation of branching fractions, we assume that the decay rates of the $\Upsilon(4S)$ to B^+B^- and $B^0\bar{B}^0$ are equal [13]. We combine branching fraction results from the two η decay channels by adding the values of $-2\ln\mathcal{L}$, adjusted for a small fit bias (see below) and taking proper account of the correlated and uncorrelated systematic errors.

In order to check the suitability of the PDFs for describing the data, we show in Fig. 2 the distribution of the likelihood ratio $\mathcal{L}(S)/[\mathcal{L}(S) + \mathcal{L}(B)]$ for the full $a_0^-(\eta_{\gamma\gamma})h^+$ sample, where $\mathcal{L}(S)$ and $\mathcal{L}(B)$ are the signal and background likelihood, respectively. Signal would appear near one in this plot but very little is seen because of the small signal yield. There is also good agreement for similar plots for the other samples. In order to show distributions of the main fit observables m_{ES} and ΔE , we require that this likelihood ratio be greater than a value that would optimize the branching fraction uncertainty, typically 0.9 for most samples. In Figs. 3 and 4 we show projections onto m_{ES} and ΔE of subsamples enriched with this requirement on the likelihood ratio (computed ignoring the PDF associated with the variable plotted).

The statistical error on the signal yield is taken as the change in the central value when the quantity $-2\ln\mathcal{L}$ increases by one unit from its minimum value. The significance is taken as the square root of the difference between the value of $-2\ln\mathcal{L}$ (with additive systematic uncertainties included) for zero signal and the value at the minimum, with other parameters free in both cases. The 90% confidence level (C.L.) upper limit is taken to be the branching fraction below which lies 90% of the total of the likelihood integral (with systematic uncertainties

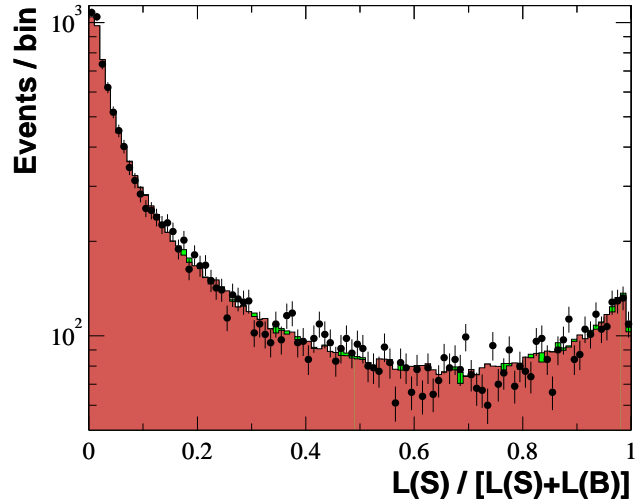


FIG. 2: The likelihood ratio $\mathcal{L}(S)/[\mathcal{L}(S) + \mathcal{L}(B)]$ for $a_0^-(\eta_{\gamma\gamma})h^+$. The points represent the on-resonance data, the solid histograms are from MC generated from background (dark shaded) and background plus signal (light shaded) PDFs.

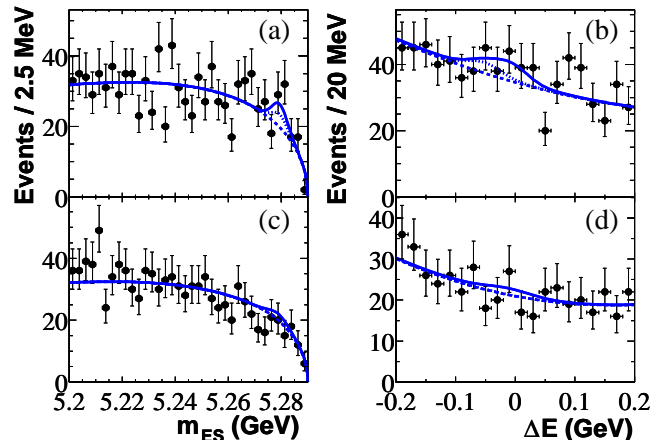


FIG. 3: Projections of the B -candidate m_{ES} and ΔE for (a, b) $a_0^-h^+$, and (c, d) $a_0^0h^+$. Points with errors represent data, solid curves the full fit functions, dashed curves the background functions (the peaking $B\bar{B}$ background component is negligible), and the dotted curve shows the kaon portion of the signal. These plots are made with a minimum requirement on the likelihood and thus do not show all events in the data samples.

included) in the positive branching fraction region.

Most of the yield uncertainties arising from lack of knowledge of the PDFs have been included in the statistical error since most background parameters are free in the fit. Varying the signal PDF parameters within their estimated uncertainties, we determine the uncer-

TABLE I: Signal yield, detection efficiency ϵ , daughter branching fraction product ($\prod \mathcal{B}_i$), significance (including additive systematic uncertainties, taken to be zero if corrected yield is negative), measured product branching fraction (see text), and the 90% C.L. upper limit on this branching fraction.

Mode	Yield	ϵ (%)	$\prod \mathcal{B}_i$ (%)	Signif.	$\mathcal{B}(10^{-6})$	UL(10^{-6})
$a_0^-(\eta\gamma\gamma)\pi^+$	18^{+11}_{-10}	18.8	39.4	1.3	$2.3^{+1.7}_{-1.5} \pm 0.9$	
$a_0^-(\eta_{3\pi})\pi^+$	15^{+9}_{-8}	15.5	22.6	1.6	$3.9^{+2.9}_{-2.5} \pm 1.0$	
$a_0^-\pi^+$				2.0	$2.8^{+1.5}_{-1.3} \pm 0.7$	< 5.1
$a_0^-(\eta\gamma\gamma)K^+$	2^{+6}_{-4}	17.9	39.4	0.1	$0.0^{+0.9}_{-0.6} \pm 0.3$	
$a_0^-(\eta_{3\pi})K^+$	13^{+8}_{-6}	14.9	22.6	1.1	$3.1^{+2.5}_{-2.1} \pm 1.9$	
$a_0^-K^+$				0.4	$0.4^{+1.0}_{-0.8} \pm 0.2$	< 2.1
$a_0^-(\eta\gamma\gamma)\bar{K}^0$	-12^{+8}_{-6}	21.4	13.5	0.0	$-3.7^{+2.9}_{-2.3} \pm 0.9$	
$a_0^-(\eta_{3\pi})\bar{K}^0$	0^{+7}_{-5}	15.8	7.9	0.5	$2.7^{+6.1}_{-4.4} \pm 1.9$	
$a_0^-\bar{K}^0$				0.6	$-1.5^{+2.4}_{-1.8} \pm 0.8$	< 3.9
$a_0^0(\eta\gamma\gamma)\pi^+$	17^{+11}_{-9}	12.8	39.4	1.4	$3.1^{+2.4}_{-2.0} \pm 1.2$	
$a_0^0(\eta_{3\pi})\pi^+$	1^{+8}_{-6}	9.5	22.6	0.3	$1.2^{+3.9}_{-3.2} \pm 1.7$	
$a_0^0\pi^+$				1.4	$2.6^{+2.0}_{-1.7} \pm 1.0$	< 5.8
$a_0^0(\eta\gamma\gamma)K^+$	0^{+5}_{-3}	12.4	39.4	0.3	$0.3^{+1.1}_{-0.6} \pm 0.4$	
$a_0^0(\eta_{3\pi})K^+$	6^{+7}_{-5}	9.1	22.6	0.5	$1.9^{+3.8}_{-2.9} \pm 2.5$	
$a_0^0K^+$				0.4	$0.4^{+1.1}_{-0.7} \pm 0.3$	< 2.5
$a_0^0(\eta\gamma\gamma)K^0$	0^{+6}_{-5}	15.0	13.3	0.5	$1.4^{+3.5}_{-2.4} \pm 1.2$	
$a_0^0(\eta_{3\pi})K^0$	4^{+5}_{-4}	9.7	7.8	1.2	$6.6^{+7.8}_{-5.4} \pm 2.8$	
$a_0^0K^0$				1.0	$2.8^{+3.1}_{-2.4} \pm 1.1$	< 7.8

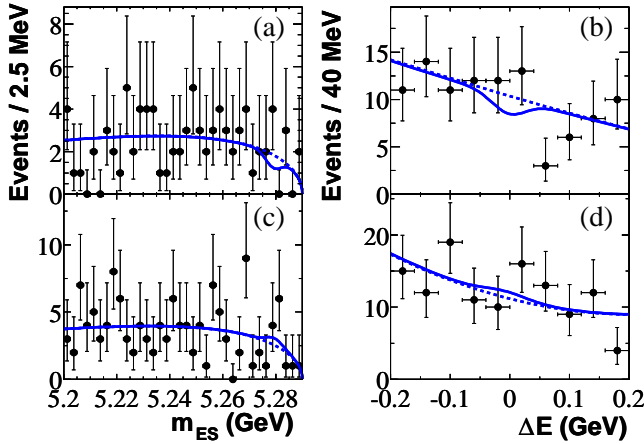


FIG. 4: Projections of the B -candidate m_{ES} and ΔE for (a, b) $a_0^- K_S^0$, and (c, d) $a_0^0 K_S^0$. Points with errors represent data, solid curves the full fit functions, and dashed curves the background functions. These plots are made with a minimum requirement on the likelihood and thus do not show all events in the data samples.

tainties in the signal PDFs to be 1–5 events, depending on the final state. The contribution to this uncertainty from the parameterization of the a_0 signal shape is small. We verify that the value of the likelihood of each fit is consistent with the expectation found from an ensemble of simulated experiments.

Uncertainties in our knowledge of the efficiency, found from auxiliary studies, include $0.8\% \cdot N_t$, $2.5\% \cdot N_\gamma$, and 4% for a K_S^0 decay, where N_t and N_γ are the number

of signal tracks and photons, respectively. Our estimate of the number of produced $B\bar{B}$ events is uncertain by 1.1%. The neglect of correlations among observables in the fit can cause a systematic bias; the correction for this bias (between -3 and $+3$ events) and assignment of the resulting systematic uncertainty (0.5–2 events) is determined from simulated samples with varying background populations. Published data [6] provide the uncertainties in the B -daughter product branching fractions (1–2%). Selection efficiency uncertainties are 0.5–3.5% for $\cos\theta_T$ and 0.5% for PID (for the $a_0 h^+$ modes).

In conclusion, we do not find significant signals for these B -meson decays to states with a_0 mesons. The measured branching fractions and 90% C.L. upper limits are given in Table I. Assuming $\eta\pi$ to be the dominant a_0 decay mode, we rule out the predictions for the decay $B^- \rightarrow a_0^- \bar{K}^0$ derived in Ref. [14].

We are grateful for the excellent luminosity and machine conditions provided by our PEP-II colleagues, and for the substantial dedicated effort from the computing organizations that support *BABAR*. The collaborating institutions wish to thank SLAC for its support and kind hospitality. This work is supported by DOE and NSF (USA), NSERC (Canada), IHEP (China), CEA and CNRS-IN2P3 (France), BMBF and DFG (Germany), INFN (Italy), FOM (The Netherlands), NFR (Norway), MIST (Russia), and PPARC (United Kingdom). Individuals have received support from CONACyT (Mexico), A. P. Sloan Foundation, Research Corporation, and Alexander von Humboldt Foundation.

* Now at Department of Physics, University of Warwick, Coventry, United Kingdom

† Also with Università della Basilicata, Potenza, Italy

‡ Also with IFIC, Instituto de Física Corpuscular, CSIC-Universidad de Valencia, Valencia, Spain

§ Deceased

- [1] Throughout this note, when we refer to a_0 , we mean specifically $a_0(980)$.
- [2] Belle Collaboration, A. Garmash *et al.*, Phys. Rev. D **65**, 092005 (2002); BABAR Collaboration, B. Aubert *et al.*, hep-ex/0308065 (submitted to Phys. Rev. D), 2003; BABAR Collaboration, B. Aubert *et al.*, hep-ex/0406040 (submitted to Phys. Rev. Lett.), 2004.
- [3] The named member of a charge-conjugate pair of particles stands for either.
- [4] S. Laplace and V. Shelkov, Eur. Phys. Jour. C **22**, 431

(2001).

- [5] V. Chernyak, Phys. Lett. B **509**, 273 (2001).
- [6] Particle Data Group, K. Hagiwara *et al.*, Phys. Rev. D **66**, 010001 (2002).
- [7] V. Baru *et al.*, Phys. Lett. B **586**, 53 (2004).
- [8] S. Teige *et al.*, Phys. Rev. D **59**, 012001 (1998).
- [9] S. Flatté, Phys. Lett. B **63**, 224 (1976).
- [10] BABAR Collaboration, B. Aubert *et al.*, Nucl. Instr. Meth. A **479**, 1 (2002).
- [11] BABAR Collaboration, B. Aubert *et al.*, Phys. Rev. D **70**, 032006 (2004).
- [12] The BABAR detector Monte Carlo simulation is based on GEANT4: S. Agostinelli *et al.*, Nucl. Instr. Meth. A **506**, 250 (2003).
- [13] See for instance BABAR Collaboration, B. Aubert *et al.*, Phys. Rev. D **69**, 071101 (2004) and references therein.
- [14] P. Minkowski and W. Ochs, hep-ph/0404194 (2004).